RUC

Antimicrobial activity of GN peptides and their mode of action

Mojsoska, Biljana; Nielsen, Hanne Mørck; Jenssen, Håvard

Antimicrobial activity of GN peptides and their mode of action

Troels Godballe[1], Biljana Mojsoska[1], Hanne M. Nielsen[2], Håvard Jenssen[1,*]

[1]Dept. of Science, Systems & Models, Roskilde University, Universitetsvej 1, DK-4000 Roskilde,

Denmark.

[2]Dept. of Pharmacy, Biologics, University of Copenhagen, Universitetsparken 2, 2100 Copenhagen,

Denmark.

*Corresponding Author: jenssen@ruc.dk Tel +45 4674 2877

Abstract

Increasing prevalence of bacteria that carries resistance towards conventional antibiotics has prompted the investigation into new compounds for bacterial intervention to ensure efficient infection control in the future. One group of potential lead structures for antibiotics is antimicrobial peptides due to their characteristics as naturally derived compounds with antimicrobial activity. In this study we aimed at characterizing the mechanism of action of a small set of *in silico* optimized peptides. Following determination of peptide activity against *E. coli, S. aureus* and *P. aeruginosa,* toxicity was assessed revealing meaningful selectivity indexes for the majority of the peptides. Investigation of the peptides effect on bacteria demonstrated a rapid growth inhibition with signs of bacterial lysis together with increased bacterial size. Both visual and quantitative assays clearly demonstrated bacterial membrane disruption after 10 minutes for the most active peptides. The membrane disrupting effect was verified by measuring the release of calcein from bacterial mimicking liposomes. This revealed the most active peptides as inducers of immediate release, indicating the kinetics of membrane permeabilization as an important determinant of bacterial activity. No well-defined secondary structure of the peptides could be determined using CD-spectroscopy in the presence of different liposomes mixtures, implying that there is no correlation between peptide secondary structure and the observed anti-bacterial and cytotoxic activity for this set of peptides. In conjunction, these findings provide strong indications of membrane disruption as the primary mechanism of bacterial growth inhibition for the tested peptides.

Keywords: Antibacterial host defence peptides; Membrane destabilization, Antibacterial mode of action; Anti-infective; b

Introduction

For a long time, the treatment of most infections in western countries has been considered a rather uncomplicated matter due to the effectiveness of various antibiotics. Fortunately that still applies, although the treatment of some bacterial infections has become gradually more complicated in recent years because of the increase in bacterial resistance against conventional antibiotics. This is made obvious by the fact that infectious diseases are the third leading cause of death in developed countries, despite the abundant availability of antibiotics [1].

The emergence of bacteria with resistance towards conventional antibiotics is increasing at an alarming rate especially in hospital settings, seriously hampering effective treatment of infections [2]. Methicillin-resistant *Staphylococcus aureus* (MRSA) was in 2005 estimated to have caused 94 000 infections leading to 19 000 deaths [3] and together with other multi drug resistant (MDR) strains of *Pseudomonas aeruginosa* and extended-spectrum-beta-lactamase (ESBL) producing *Klebisella pneumonia* and *Escherichia coli,* they pose an increasing threat to public health [4]. On top of this there has only been introduced a very limited number of new antibacterial agents to the market since the 60's which together with a rapid declining interest from medical companies into development of new antibiotics, illustrates a development that calls for concern [2, 4]. In that perspective, it is important to pursue the development of new antimicrobial agents, with a novel mode of action, to ensure that we will be able to cure life-threatening infections in the future. One such group of compounds that has the potential to assist in the fight against infections is antimicrobial peptides.

Antimicrobial peptides are a natural component of the innate immune system in a wide range of organism, acting as a first line of defense against various microbes. These peptides have been isolated from a great number of organisms ranging from bacteria to plants, invertebrates and vertebrates, thereby demonstrating their prevalence in virtually all branches of life [5]. In relation to their abundance among different kinds of organisms, the biological effect varies from direct bacterial inhibition [5] to immune modulating [6], proving their versatility as effector molecules. The variety in origin and biological effect is reflected in the characteristics of antimicrobial peptides having a great deal of diversity, in both primary and secondary structure, probably explaining their evolutionary success [7]. Even so, there are a number of structural similarities that apply for most antimicrobial peptides, usually

60   being relatively short, ranging from 12-50 amino acids, carrying a net positive charge of +2 to +9 and

61   having a distinct proportion of hydrophobic residues [8].

62   The positive charge of antimicrobial peptides is generally accepted as the main feature that mediates

63   selectivity towards bacteria by harboring sufficient electrochemical attraction towards the negatively

64   charged outer entities of bacterial cells to allow selective activity. As natural compounds with an

65   antimicrobial effect, antimicrobial peptides have drawn the attention of scientist to investigate their

66   potential as future antimicrobial agents. This has led to the identification of more than 1000

67   antimicrobial peptides [9], and numerous attempts to improve activity by modifying natural antimicrobial

68   peptides or the *de novo* design of antimicrobial peptides [10] including the use of unnatural amino acid

69   analogues [11]. Although a large number of natural and synthetic antimicrobial peptides have been

70   studied, there are still today, questions tied to the exact nature of bacterial inhibition exerted by these

71   peptides. Compiling evidence suggests that antimicrobial peptides have a plethora of effects against

72   bacteria, ranging from unspecific membrane perforation to specific inhibition of intracellular targets

73   and the bacterial inhibition exerted by some antimicrobial peptides is possibly the result of more than

74   just one isolated mechanism [5]. Although different targets have been identified, a detailed

75   characterization of the mode of action has only been carried out on a minority of peptides. To truly take

76   advantage of antimicrobial peptides and make use of their potential as lead structures for bacterial

77   intervention, it is therefore in that perspective that the scope of this work is to elucidate the mechanism

78   of action of a set of different synthetic antimicrobial peptides. The antimicrobial peptides used in this

79   study were originally designed by Fjell and colleagues by the use of *in silico* screening [12]. The 10 most

80   active peptides from this optimization were selected for investigation in this study, all having a positive

81   charge of +4, uniform chain length of 9 amino acids and at least three tryptophan residues. To verify

82   the activity of the peptides, minimal inhibitory concentration (MIC) testing was carried out against *E.*

83   *coli, P. aeruginosa and S. aureus* reference strains and the two most active peptides were selected for

84   further studies to elucidate the mechanism of bacterial inhibition. Herein we demonstrate compelling

85   evidence for membrane perforation as the main contributor of bacterial inhibition together with

86   reversible metabolic disturbance at lower concentrations.

87

Material and methods

Solid phase peptide synthesis

The peptides were synthesized using solid phase Fmoc chemistry with amidation on the carboxyl end, purified by reverse-phase HPLC using a C_{18} column (Higgins Analytical Inc. 10 μm 250x10 mm) and a water/acetonitile gradient. The correct mass and purity >95% was verified using Dionex Ultimate 3000 RP-UHPLC (C18 Kinetex 100 x 2.1 mm, 100 Å) electrospray ionization mass spectrometry (Finnigan LTQ) (**Figure S1, Table S1**).

Minimal inhibitory concentration determination

The antimicrobial efficacy of peptides was tested using a serial dilution titration, as previously described [13] on a panel of clinically relevant bacterial strains; i.e. *E. coli* (ATCC 25922), *P. aeruginosa* PAO1 (ATCC 15692), *S. aureus* (ATCC 29213). Conventional antibiotics used throughout the study include Ampicillin (A9518), Ciprofloxacin (17850), Tetracycline (T7660), Tobramycin (T4014) and Polymyxin B (92301), all purchased from Sigma. In short, overnight cultures were grown to mid-log phase before diluting to ~5×10^5 CFU/mL in Mueller Hinton broth (Becton Dickinson) and 90 μL was used to inoculate each well of a 96-well polypropylene plate (Cat. No. 3879, COSTAR). Then, 10 μL aliquots of a 2-fold dilution series of the peptides were added and the minimal inhibitory concentration (MIC) was scored as the lowest concentration that inhibited visible growth after 48 hours of incubation at 37°C.

Hemolysis assay

Freshly drawn human blood with EDTA as anticoagulant was washed and centrifuged at 500 g for 5 minutes until the appearance of clear supernatant. A two-fold dilution series of peptides was added to 96-well polypropylene microtiter plates (COSTAR Cat. No.3879) in 75 μL aliquots together with 50 μL of 4 % final concentration of red blood cells (RBC) giving a total volume of 125 μL. The plate was incubated with shaking for 1 hour at 37°C, before being centrifuged at 250 g for 5 minutes. 50 μL of the supernatant was diluted 1:3 in sterile saline in a flat bottomed 96-well greiner plate before

115 measuring absorbance at 414 nm, using a multi-detection microplate reader Synergy HT. 100 % lysis

116 was defined as RBC treated with 1% Triton-X 100 and sterile saline treated RBC was added for

117 baseline adjustments. The test range was 3.1-400 µg/mL.

118

119 **MTT assay**

120 Toxicity against HeLa cells was estimated by the MTT viability assay. HeLa cells were cultured in

121 DMEM Glutamax media (32430-027, Invitrogen), media supplemented with 10% FBS and 1%

122 pen/strep using standard techniques. The cells were passaged at least 2 times before being used in the

123 assay, to ensure logarithmic growth. At 80 % confluency, cells were harvested, quantified and 10.000

124 cells/well were seeded in a 96-well microtiter plate. The cells were placed in a humidified 5% CO_2

125 atmosphere at 37°C for 24 hours. Media was aspirated and the cells were washed with PBS w/o Ca^{2+}

126 and Mg^{2+}. A mixture of peptide and DMEM media (100 µl) was added and the cells were incubated in

127 a humidified 5% CO_2 atmosphere at 37°C for 1 hour before wash with PBS with or without Ca^{2+} and

128 Mg^{2+}. MTT (50 µg) dissolved in PBS with or without Ca^{2+} and Mg^{2+} was added and the cells were

129 incubated 90 minutes in a humidified 5% CO_2 atmosphere at 37°C. MTT solution was aspirated and

130 100 µL of DMSO was added to dissolve the formazan crystals before incubating 5 minutes at 37°C.

131 The absorbance at 540 nm was read in a multi-detection microplate reader Synergy HT. Viability

132 control was assigned to samples with only HeLa cells and DMEM media and 0 % viability was

133 assigned to samples with 1 % added Triton-X-100 instead of peptides. The assay was done 3 times with

134 duplicates and results are the mean of these. Concentrations giving a 50% reduction in metabolism

135 (IC_{50}), was calculated using equation (I) in Graphpad Prism.

136 $$Y = \frac{100}{1+10^{((LogIC50 \div X) \cdot HillSlope)}}$$ (Eq. I)

137

138

Killing kinetics

Colony forming units (CFU) counts were monitored for 180 minutes, following peptide exposure at concentration corresponding to 1×, 2× and 4×MIC. Overnight culture of *E. coli* ATCC 25922 was diluted with fresh Mueller Hinton broth and re-grown to mid-log phase before diluting to a turbidity of OD_{600} 0.1 and loading 90 µL into wells of a flat bottomed 96-well Greiner plate containing 10 µL of peptides solution. Growth control was assigned to wells without peptide. The content of individual plates was collected and plated out in duplicate on LB agar plates. Between extractions, the microtitter plate was sealed and placed at 37°C. LB agar plates were incubated for 18 hours at 30°C and colonies were counted. The presented results are the mean of 3 independent experiments.

The effect of peptides on bacterial growth was investigated by monitoring optical density (OD) following peptide exposure. Overnight culture of *E. coli* ATCC 25922 was diluted with fresh Mueller Hinton broth and re-grown to mid-log phase before diluting to a turbidity of OD_{600} 0.1. A microtiter plate was filled with 10 µL of peptide or antibiotic solution per wells, before loading 90 µL of bacterial suspension. For both peptides and antibiotics, concentrations corresponding to 1×-, 2×- and 4×MIC were used. OD_{600} was measured, with a multi-detection microplate reader Synergy HT at 37°C, every 8 minutes for 5 hours with shaking. The readings were baseline corrected against wells with only Mueller Hinton broth. Comparison between a standard spectrophotometer, with a cuvette length of 1 cm, and the readings obtained from the plate reader showed a difference with 5-fold lower readings from the plate reader (data not shown). In order to make readings meaningful, in relation to the correlation between optical density and concentration of bacterial cells, the readings from the plate reader was multiplied with a factor of 5.

The effect on both bacterial DNA content and change in cell size after exposure with peptides was monitored over 180 minutes by flow cytometry. An overnight culture of *E. coli* ATCC 25922 was diluted with fresh Mueller Hinton broth and re-grown to mid-log phase before diluting to a turbidity of OD_{600} 0.1. A total of 90 µL of this bacterial suspension was loaded into a flat bottomed 96-well Greiner plate for peptide and antibiotic samples and 100 µL for control samples. After extraction of the zero sample, 10 µL of peptide solution corresponding to 1× and 4× the MIC concentration was added for a total volume of 100 µL. Two wells were loaded for each treatment to ensure enough bacteria for the

167 flow cytometry analysis. Immediately after extraction the samples were put on ice and centrifuged at 10

168 000 g for 5 minutes at 4°C and resuspended in 100 µL 10 mM Tris HCl pH 7.4 before fixing with 1000

169 µL 77% ethanol. The following day, the samples were centrifuged at 10 000 g for 5 minutes before

170 gently removing the supernatant and adding 140 µL staining solution (90 µg/mL Mitramycin and 20

171 µg/mL ethidium bromide in 10 mM Tris pH 7.4, 10 mM $MgCl_2$). The samples where run on an A10

172 Bryte Flow Cytometer and when possible, 20 000 events were included in the analysis.

173

Membrane depolarization assay

175 The LIVE/DEAD® BacLight ™ Bacterial Viability Kit (L7012, Invitrogen), was applied to peptide

176 treated *E. coli* ATCC 25922, to investigate a visual indication of the membrane permeability

177 capabilities of the peptides. Overnight culture of *E. coli* ATCC 25922 was diluted with fresh Mueller

178 Hinton broth and re-grown to mid-log phase before diluting to a turbidity of OD_{600} 0.1. Then 10 µL of

179 peptide solution corresponding to a final test concentration of 1× and 4×MIC was added to a flat

180 bottomed polystyrene Greiner plate before loading 90 µL of bacteria suspension. 100 µL of bacterial

181 suspension was used as a control. Each well corresponded to one time point for each individual

182 treatment. The plate was placed at 37°C and the samples were extracted at the indicated time points and

183 immediately put on ice. The samples were then centrifuged at 10 000g for 5 minutes, and the pellet

184 resuspended in 100 µL 0.9% ice cold NaCl, to remove interfering media components. Staining solution

185 (1 µL) was added and incubated for 15 minutes in the dark, before loading to 1% agarose slips on

186 microscope slides. Staining solution was prepared by adding 5 µL of 3.3 mM Syto-9 dye in DMSO

187 (Compound A) and 5 µL of 20 mM Propidium iodide in DMSO (Compound B) to 20 µL of sterile

188 water. Samples were inspected with a Leica DM5000B microscope using a mercury lamp. A filter cube

189 with excitation filters of 436, 495 and 580 nm and emission filters of 460, 535 and 630 nm was used to

190 be able to detect both live and dead bacteria.

191 To verify the findings from microscope pictures with an assay that could characterize the membrane

192 permeability of the entire bacterial population in the samples, the Live/Dead quantification was

193 performed. The assay was essentially performed according to the manufacturer's instructions. After

194 establishing a standard curve from known ratios of isopopyl killed and live bacteria an overnight

195   culture of *E. coli* ATCC 25922 was diluted with fresh Mueller Hinton broth and re-grown to mid-log

196   phase before diluting to a turbidity of OD_{600} 0.1. The bacterial solution and peptide solution was mixed

197   in a 9:1 ratio (vol/vol) in a 96-well polypropylene plate (Cat. No. 3879, COSTAR) and incubated at

198   37°C. At the indicated timepoints the content of individual wells was extracted, put on ice and then

199   pelleted at 11 000 g for 8 minutes before being resuspended in 0.9% NaCl and placed on ice again. The

200   resuspended bacterial suspension was then added to individual wells of flat bottomed 96-well

201   polystyrene plate and mixed with 100 µL staining solution before incubation in the dark for 15 minutes

202   and subsequent measurement of fluorescence on a multi-detection microplate reader Synergy HT.

203   Green fluorescence was excited at 485 nm and the emission detected at 528 nm, whereas the red

204   fluorescence was excited at 530 nm and detected at 645 nm. Percentage of living cells was obtained by

205   using equation (II) using the standard curve made from known ratios of live cells. The staining solution

206   was prepared by adding 3 µL of both compound A and B, for each 1 mL of distilled sterilized water

207   and stored in the dark.

208

$$\% \text{ live cells} = \frac{\textit{Green fluorescence}}{\textit{Red fluorescence}} \cdot \frac{1}{0.0627} \qquad \text{(Eq. II)}$$

209   **Liposome preparation**

210   Large unilamellar vesicles (LUVs) was prepared by mixing POPC (1-palmitoyl-2-oleoyl-sn-glycero-3-

211   phosphocholine) and POPG (1-palmitoyl-2-oleoyl-sn-glycero-3-phosphoglycerol) and in a molar ratio

212   of 3:7 as a simple mimic of bacterial membranes and POPC:POPG:Cholesterol was mixed in a molar

213   ratio of 5:2:3 as a simple mimic of mammalian membrane. POPC (770557), POPG (770257) and

214   Cholesterol were all purchased from Avanti Lipids (Alabaster, Alabama). The lipid mixture was

215   concentrated on a rotary evaporator and washed 3 times with 99.9 % ethanol to remove residual

216   organic solvents. The lipid mixture was then dissolved in 4 mL HEPES buffer (10 mM HEPES, 150

217   mM KCl, 0.03 mM $CaCl_2$, 0.01 mM EDTA, pH 7.4) with 20 mM calcein (C0875, Sigma), for calcein

218   containing liposomes and 10 mM Tris pH 7.4 for empty liposomes used for CD spectroscopy, followed

219   by thorough mixing and sonication for 5 minutes to prevent aggregates. Subsequently, the lipid mixture

220   was vigorously whirlmixed every 10 minutes over the course of 1 hour and finally left at room

221   temperature for 1 hour, to allow the lipids to anneal. LUVs were prepared by extruding the lipid

222   mixture through, two double stacked 100 nm filters, a total of 10 times using a Nitrogen powered

223   extruder. The calcein containing liposomes were loaded on Sephadex G-50 columns to separate

224   encapsulated calcein from free calcein and eluted with HEPES buffer. The size of the liposomes was

225   verified to be approximately 110 nm with a narrow size distribution by dynamic light scattering (DLS)

226   using a Zetasizer Nano ZS (Malvern, Worcestershire, UK). Malvern DTS v. 5.10 software (Malvern,

227   Worcestershire, UK) was used for acquisition and analysis. By comparing the end volume with the

228   starting volume, the dilution of the initial liposome concentration was estimated and that lead to the

229   anticipation of a stock concentration of 971 µM of the liposomes.

230

231   **Calcein release assay**

232   Calcein release was done in a 96-well plate with shielded wells (MicroWell 96 optical bottom plate,

233   NUNC, Roskilde, DK). 100 µL of peptide diluted in 10 mM HEPES buffer was added and immediately

234   before measurement of leakage, 80 µL of 45 µM liposome suspension was added for a final liposome

235   concentration of 20 µM. The liposome concentration was calculated from the starting concentrations of

236   lipids, taking into account the change in volume during preparation, and assuming a 100% yield from

237   the sephadex column. Measurements were performed in a FLUOstar OPTIMA plate reader at an

238   excitation wavelength of 485 nm and an emission wavelength of 520 nm over the course of 1 hour at

239   37°C. Maximum leakage of liposomes was acquired by lysis with 10% Triton and release following

240   peptide exposure, was calculated using equation (III), where F_{max} denotes fluorescence after addition of

241   10% Triton, F_0 represents background fluorescence of liposomes and F designates the fluorescence

242   intensity after peptide addition.

243
$$\% \ leakage = 100 \bullet \left(\frac{F - F_0}{F_{max} - F_0} \right)$$
(Eq. III)

244

245 **Results**

246 This study aimed at characterizing the bacterial inhibition and antibacterial mode of action of a set of

247 highly active antimicrobial peptides earlier identified by Fjell *et al.* [12]. The GN peptide library was

248 screened for antibacterial activity against Gram-negative *E. coli* ATCC 25922 and *P. aeruginosa*

249 ATCC PAO1 and Gram-positive *S. aureus* ATCC 29213 bacteria. The minimal inhibitory

250 concentrations of the tested peptides demonstrated a significant spread in activity pattern from 1.5 to

251 100 μg/mL (**Table 1**). Potent broad spectrum activity against both Gram-negative and Gram-positive

252 bacteria was observed for GN-2, GN-4 and GN-6 peptides. For specific activity against *E. coli*, GN-14

253 exhibits as good antimicrobial activity as GN-2, GN-4 and GN-6 peptides. Similarly, a pronounced

254 antimicrobial activity against *S. aureus* was observed for GN-5 peptide (1.5 μg/mL), and GN-2 and

255 GN-6 peptides (3.1 μg/mL). However, in respect to a broad spectrum antimicrobial potential, peptide

256 GN-2 and GN-4 appear as best candidates.

257 In an attempt to explain the antibacterial peptide properties with classical chemical properties the

258 hydrophobic moment was measured for all the peptides. This quantitative measure of the peptides

259 amphipathicity indicates that antibacterial activity increases proportionally with the hydrophobic

260 moment (**Table 1**). In order to further characterize the antimicrobial profiles of the GN peptides, their

261 ability to selectively target bacterial- versus mammalian cells was assessed using hemolytic assay.

262 Human red blood cells were exposed to different concentrations of GN peptides and the degree of lysis

263 was evaluated. All peptides resulted in a dose dependent release of hemoglobin, and toxicity is reported

264 as the highest concentration of peptides resulting in less than 10 % lysis compared to PBS treated

265 control cells (**Table 1**). Comparing antibacterial and hemolytic potential, the peptide library clearly

266 separates into two sub-groups; GN-8, -9, -11 and -12 being hardly hemolytic with low antimicrobial

267 potential, while the remaining peptides demonstrate an overall higher antibacterial effect yet still only

268 modest hemolytic activity. Thus, for this set of peptides the tendency to lyse human red blood cells is

269 highly correlated with the ability to kill bacteria. In comparison, indolicidin, a small 13 amino acids

270 tryptophan and arginine rich antimicrobial peptide[14], is used as an antibacterialreference peptide

271 indicating that most of the GN peptides have superior selectivity. To further complement the

272 assessment of the potential toxicity of the GN peptides, a MTT assay was performed on HeLa cells and

273 the inhibitory concentrations giving 50 % reduction (IC_{50}) of cellular metabolic activity were calculated

274   (**Table 1**). The results are in agreement with the hemolytic activity, thus demonstrating that the

275   peptides with the highest antimicrobial activities are the peptides exhibiting the greatest metabolic

276   inhibition in HeLa cells. Hence, peptides GN-2 and GN-4 stand out as most cytotoxic with IC_{50} values

277   of 47 and 37 μg/mL, respectively.

278   To dissect the antimicrobial activity of GN peptides with a range of different assays, GN-2 was chosen

279   as the most potent peptide with good selectivity index range of 16 to 32. Correspondingly, GN-6 which

280   structurally differs from GN-2 peptide in the presence of phenylalanine and a patch of 4 consecutive

281   tryptophan residues was also considered for characterization for the mechanism of bacterial inhibition.

282   First to differentiate between bactericidal or bacteriostatic mode of antibacterial activity, colony

283   forming unit counts were monitored for *E. coli* cultures exposed to 1×, 2×, and 4×MIC concentrations

284   of GN-2 and GN-6 peptide. This assay illustrated the ability of the different peptide concentrations to

285   reduce the colony forming unit counts over a period of 180 minutes. The GN-2 peptide demonstrates

286   fast antimicrobial activity indicated by a decrease of exponentially growing bacteria within the first 40

287   minutes of exposure (**Figure 1**). The inhibition proceeds for 80 minutes after which there is a

288   reestablished bacterial growth observed. Similar pattern is observed for GN-6 peptide with a slightly

289   delayed inhibition. Bacterial inhibition is concentration dependent for both peptides, even though the

290   standard error bars for GN-6 peptide at 4×MIC show high experimental variation.

291   To further elucidate the bacterial inhibition exploited by the peptides, bacterial mass was monitored by

292   optical density readings at 600 nm over a course of 5 hours. The control bacteria display exponential

293   growth until 120 minutes after which clear decrease in optical density is observed. There is a

294   reestablished growth after 180 minutes, indicating that the decrease after 2 hours is not due to limited

295   nutrition and/or waste build-up (**Figure 2**). A number of antibiotics were analyzed in parallel for

296   growth inhibition patters so that the potential bacterial targets of GN-2 and GN-6 peptides could be

297   elucidated. In addition to the viability experiments of exponentially growing *E. coli*, the optical density

298   measurements revealed clear concentration dependent inhibition of the optical density readings when

299   bacteria were exposed to 1×MIC concentration of both GN-2 and GN-6 peptide when compared to the

300   untreated bacteria. The inhibition is most pronounced at 2×MIC concentration for both peptides. With

301   respect to 1×MIC concentration of both peptides, the inhibition pattern is different indicating distinct

302   ways of exerting antimicrobial activity halting bacterial growth. Both peptides at 2×MIC concentration

303   demonstrate low OD measurements indicative of some degree of bacterial lysis.

304   Flow cytometry analyses were used to characterize the effect of GN-2 and GN-6 peptide on cell size

305   and DNA content. Exponentially growing *E. coli* were exposed to 1× and 4×MIC concentrations of

306   GN-2 and GN-6 peptides and samples were analyzed every 20 minutes over a course of 3 hours for

307   DNA content per cell mass extrapolated by fluorescence/lightscatter measurements. Untreated *E. coli*

308   show fairly constant ratio of DNA per cell size indicative for a healthy growing bacterial population.

309   Exposure to 1× and 4×MIC concentration of GN-2 gives pronounced initial decrease of DNA content

310   per cell size as compared with the control samples. After 40 minutes of exposure an increase of DNA

311   per cell size is observed for samples treated with 4×MIC concentration, referring to the reestablishing

312   of the DNA content at this point. At 120 minutes the effect of DNA content per cell size follows similar

313   ratio to that of the control, indicating a possible recovery (**Figure 3A**). Similar fashion of initial fast

314   and persistent decrease of DNA per cell size followed by an increase after 40 minutes is observed for

315   bacteria treated with 1×MIC concentration of GN-6 peptide.

316   The increase in cell size indicated by the lightscatter measurements observed in the flow cytometry

317   data (**Figure S2**) is supported by the microscopy images taken at time zero and 180 minutes for the

318   control *E. coli* population. Bacteria treated with GN-2 peptide at 1× and 4×MIC concentration appear

319   slightly bigger in size than the control bacteria. Clear difference between cells treated with 1× and

320   4×MIC concentrations of GN-2 peptide is observed by the large areas of cell debris and bacteria

321   transparency indicating cell lysis in samples treated with 4×MIC (**Figure 3C**). Upon treatment with

322   GN-6 peptide at 4×MIC concentrations, there is a clear morphological change presented by cells that

323   appear long and filamentous but not lysed (**Figure 3C**). This data is in agreement with the observations

324   from the flow cytometry analyzes on DNA, size and DNA /size.

325   Live/dead staining experiments with SYTO9 green-fluorescent nucleic acid stain and propidium iodide

326   red-fluorescent stain, were used to analyze the membrane permeability capacity of GN-2. Under

327   conditions where no membrane permeabilizing agent is present, bacteria with intact membranes will

328   stain green (**Figure 4A**). The un-treated control cells are naturally predominantly staining green at all

329   time-points, illustrating a healthy population of bacteria. *E. coli* exposed to GN-2 peptide at 1×MIC

330   concentration at the 10 and 20 minutes time-point, demonstrate about 90 % permeabilized membranes,

331   thus staining red. However, over time the surviving cells are replicating, resulting in an increasing

332   percentage of green cells in the later time points (**Figure 4B**). Upon increasing the GN-2 peptide

333   concentration to 4×MIC, the membrane integrity stays disrupted throughout the assay of 120 minutes

334   (**Figure 4C**). To quantify the membrane permeability in a more un-biased fashion than microscopy, the

335   same bacterial cultures were also analyzed using a multi-detection fluorescence plate reader. Plotting

336   the ratio of live and dead cells for cultures incubated with 1×, 2× and 4×MIC concentration of GN-2

337   peptide over time, clearly demonstrates how 2× and 4×MIC knocks down the viability to around 20%

338   and this level is kept for 120 minutes. Contrary, at 1×MIC of GN-2, the level of viable bacteria after 10

339   minutes is about the same as in the samples treated with 2× and 4×MIC of GN-2, but at 1×MIC the

340   culture re-growths with a doubling time of about 1 hour (**Figure 4D**).

341   Due to previously established observation of membrane disruption as a primary mode of action of the

342   GN peptides, calcein leakage assay was performed. This assay allows characterization of peptides

343   based on the different potencies to provoke membrane leakage of calcein entrapped unilamellar

344   phospholipid vesicles (LUVs) made of POPC:POPG (3:7 molar ratio). Calcein is a self-quenching

345   molecule that at high concentration shows relatively low background fluorescence. As calcein

346   molecules are being released to the exterior of the vesicles, the fluorescence increases. The percentage

347   of calcein leakage can be plotted as a function of the concentration of the peptides. All GN peptides

348   were able to induce calcein leakage in a concentration dependent manner at endpoint reading of 60 min

349   (**Figure 5A**). But the release of calcein is much less significant that what is induced by melittin, a well-

350   known peptide with non-selective lytic properties, used as a positive control for giving distinct pattern

351   of liposome disruption [15].

352   As it was impossible to distinguish the lytic potential of the different GN peptides using an endpoint

353   reading the release of calcein over time was monitored, enabling us to extract information about the

354   capability of the peptides to induce calcein leakage. The GN-2 peptide demonstrates distinct kinetics of

355   rapidly provoking calcein release from the liposomes, particularly at high concentrations (**Figure 5B**).

356   Only a small concentration change from 3.5 µg/mL to 5.5 µg/mL of GN-2, changes the calcein release

357   from about 30% to 100%. Conversely, the GN-6 peptide, which has slightly lower antimicrobial

358   activity than GN-2, exerts a much more gradual release of calcein over time, which stabilizes after

359   about 10 minutes (**Figure 5C**). The gradual release is observed for a wider range of concentrations,

360   suggesting different mode of membrane activity or different modes of action for this peptide compared

361   to GN-2. This could potentially be reconfirmed and better characterized using the experimental design

362   of Russel *et al.* 2010 [16]. A similar, but even more dramatic profile for gradual release is observed for

363   GN-14 where gradual increase in calcein leakage progressing over a course of 20 minutes is observed

364   (**Figure 5D**). The different patterns of calcein leakage attribute to the correlation of antimicrobial

365   peptide activity and their ability to disrupt bacterial membranes, where more active peptides cause

366   more instantaneous release of calcein from the liposome.

367   The secondary structure of GN peptides and melittin was inspected with circular dichroism (CD)

368   spectroscopy to see whether or not a confined structure is necessary for the antimicrobial, toxic or

369   membrane disrupting activities observed. Peptide secondary structures were measured in Tris buffer pH

370   7.4 and unilamellar phospholipid vesicles consisting of POPC:POPG:Cholesterol (5:2:3 molar ratio)

371   and POPC:POPG (3:7 molar ratio), the latter mimicking mammalian and bacterial membranes,

372   respectively (**Figure S3**). None of the peptides demonstrated any defined secondary structures in Tris

373   buffer, indicating random coils under these conditions. In presence of LUV that mimic mammalian

374   membranes, the control peptide melittin adopts a structural confirmation similar to that of an α-helix

375   with peak minima at 222 and 208 nm [17]. Using the DichroWeb K2D algorithm [18], the α-helix content in

376   melittin was calculated to be 77 % which is in agreement with other publications [19]. The CD spectra for

377   the GN peptides are similar for mammalian and bacterial membrane mimics and illustrate no well-

378   defined secondary structure in either environment. Therefore, it is reasonable to assume that GN

379   peptides exert their antimicrobial, toxic and membrane disrupting activity without adapting any well-

380   defined secondary structure.

381

382

383   **Discussion**

384   Due to the increased number of infectious agents that are resistant to many well-known classes of

385   antibiotics, there is a constant need of improved alternative drug classes and therapies. In this study we

386   present evaluation of the antimicrobial potencies of ten different peptides, GN-2 to GN-14, from the *in*

387   *silico* optimized peptide library previously reported on by Fjell *et al.* [12]. These peptides are rich in

388   tryptophan residues along with lysine and arginine in various orders along the backbone (**Table 1**). The

389   contribution of the arginine, lysine and tryptophan residues to the antimicrobial activity is exerted by

390   primary interaction of the charged residues with the net negative charge distributed on the surface of

391   the bacterial membranes followed by insertion of tryptophan residues in the interfacial region of the

392   phospholipid bilayer [20]. Beneficial features within the GN peptide library that exhibit somewhat higher

393   antimicrobial activity than others are the cationic and bulky three residues in the amino terminal with

394   specific annotation to the cationic residues which mediate interaction with the anionic lipids and lead to

395   membrane instability in Gram-negative bacteria models [21]. This observation is further supported with

396   the GN peptides -8, -9, -11 and -14 which have either leucine or isoleucine in addition to one cationic

397   (either lysine or arginine) and one tryptophan residues within their structure and exhibit lower

398   antimicrobial activities.

399   To understand the overall activity of the GN peptides and their ability to selectively discriminate

400   between bacterial and mammalian membranes, and therefore obtain a selectivity index as a ranking tool

401   for the most potential peptide candidate, hemolytic and toxic effects were investigated. A strong

402   relationship between hydrophobicity and high antimicrobial activity and high toxicity has been reported

403   in the literature[22]. Such observation could not be observed in this study for the GN peptides. GN-2 and

404   GN-4 are the most active against both Gram-positive and Gram-negative bacteria and have both high

405   hemolytic profiles. They share the same charge distribution along their backbone differing only in

406   isoleucine (GN-2) and leucine (GN-4) at the C-terminal end and arginine (GN-2) and lysine (GN-4) at

407   the 4th position. The last feature suggests that the lysine residue in GN-4 peptide, which is previously

408   ascribed as a contributor to the higher lytic effects [21], exerts the same effect when compared to arginine

409   in GN-2 peptide (**Table 1**).

410   For a better differentiation of host cell toxicity, metabolic activities in HeLa cells were also monitored.

411   Comparing toxicity against HeLa cells with the hemolytic properties of the GN peptides, reveals a

412   disproportionally high toxicity towards the former (**Table 1**). This could be related to the peptides

413   exerting higher selectivity to the more anionic cancer cells, similar to previous observations [23]. In

414   addition, peptides that successfully entered HeLa cells could target intracellular membranes that

415   resemble bacterial membrane such is the mitochondrial membrane and therefore inhibit metabolism

416   that could be lethal to eukaryotic cells [24]. To further elucidate the observed toxicity of GN-2 and GN-4,

417   peptides toxicity measurements on a non-cancerous mammalian cells or animal studies should be

418   employed.

419   The current study demonstrate a fast decrease of exponentially growing *E. coli* when exposed to sub-

420   MIC concentrations of both peptide GN-2 and GN-6 (**Figure 1 and 2**). The observed decrease is

421   probably due to metabolic disturbance that halts bacterial growth for about 80 minutes, after which the

422   growth is reestablished. This is also in agreement with the OD measurements, which revealed similar

423   decrease in the bacteria growth under the same conditions. Flow cytometry analysis show that over a

424   period of 80 minutes the cell size at MIC concentrations does not change significantly, thus supporting

425   the above stated evidence (**Figure S2**). In support of this, the microscopic images reveal no obvious

426   morphological difference except that the MIC treated samples appear slightly bigger in size. The

427   increase in cell size is a result of metabolic inhibition which delays the decrease in cell size which is

428   normally observed when bacterial suspension gets denser [25]. In contrast to the bacteriostatic inhibition

429   at MIC concentration of both the GN-2 and GN-6 peptide, bactericidal inhibition is observed at 4×MIC

430   concentrations. Inhibition through bacterial lysis is ascribed to GN-2 peptide which causes decrease in

431   OD of *E. coli* over time, and such relationship has also been described in the literature [26]. The

432   mechanism behind the bactericidal killing for GN-6 demonstrates no signs of lysis rather than

433   filamentation which are reported as an increase in the lightscatter from the flow cytometry analysis [27].

434   These results are further corroborated by the microscopy studies. Prior studies have shown that the SOS

435   response to ciprofloxacin and beta-lactams is ascribed to filamentation [28] and the same can be induced

436   by multiple environmental stresses [29].

437   Disturbed membrane integrity of *E. coli* is observed after 10-20 minutes of exposure of 1×MIC

438   concentration of GN-2 peptide, followed by gradual reestablishment or growth of cells that survived

439   the initial attack (**Figure 4**). The latter seems plausible as cells surviving exposure to the peptide would

440   be in a rough and rather hostile environment, thus explaining their very slow growth. The phenomena

441   observed between 40 and 80 minutes, does also correlates with the observations of constant cell size

442   from flow cytometry analysis and a standstill in CFU. However, using live/dead staining analysis the

443   reestablishment of membrane integrity has been ascribed to membrane reassembly which leads to

444   propidium iodide exclusion [30] or possible efflux pumps that drive propidium iodide out of the cell [31].

445   The later mechanism would require presence of ATP for efflux pumps which could be in agreement

446   with membrane leakage and escape of ions upon peptides acting on membranes at low concentrations,

447   provoking ATP production [32]. In summary, it may seem as GN-2 induce sufficient membrane

448   permeabilization for the entry of propidium iodine, but the process does not translate into full loss of

449   viability. In relation to this observation, prior studies have shown that Bac8c, a peptide with sticking

450   resemblance to the GN peptides, can causes membrane depolarization after 5 minutes of exposure

451   followed by membrane recovery after 90 minutes [33]. In case of 2× and 4×MIC concentrations of GN-2

452   peptide, the peptide consistently causes membrane leakage supported by the visual and quantitative

453   membrane leakage assays supported by CFU counts that show loss of bacterial viability (**Figure 3 and**

454   **4**).

455   The GN-2 peptide with a very narrow concentration range from 5.5 to 1.7 µg/mL induced instant

456   release of calcein from model membranes, corresponding to 100% and 5%, respectively (**Figure 5**).

457   This observation coincides with a proposed model of membrane active antimicrobial peptides binding

458   to the surface of the phospholipids parallel to the membrane (S-state) and upon reaching a threshold

459   change their orientation into perpendicular position (I-state), thereby inducing a more profound

460   membrane disruption [32]. The GN-14 peptide revealed a more gradual release of calcein content which

461   progresses over a period of 20 minutes. Such release has been ascribed to a mechanism of transient

462   pore formation [34] where liposomes re-stabilize resulting in plateau state of calcein release [34-35], leaving

463   partially depleted liposomes. Given that the GN peptides only are composed of 9 amino acids, the

464   toroidal pore model is the more plausible mechanism of membrane action due to the fact that the pores

465   in this model are stabilized by both lipids and peptides rather than only peptides as in the barrel-stave

466   model [34]. A membrane mechanism involving toroidal pores are further supported by the lack of well

467   defined secondary structures in the GN peptide library (**Figure S3**), and none helical peptides have also

468   by others been demonstrated to work through this mechanism [36].

469   Previous studies have shown that melittin is a pore forming membrane active peptide that acts in an all

470   or none manner [19c, 37], resulting in these immediate release profiles of calcein. Since the current study

471   showed similar kinetics in mediating calcein release for both melittin and GN-2, it is reasonable to

472   assume that the GN-2 peptide also acts by pore formation mechanism. However the calcein release for

473   mellitin is much more pronounced at lower concentrations when compared to the release for peptide

474   GN-2 Fig.5A. Having said that it is important to stress out that melittin and GN-2 act with different

475   potencies of 16.3 (3.5 µg/mL) lipid/peptide molar ratio for melittin and 5.4 (5.5 µg/mL) for the GN-2

476   peptide. Furthermore, we would argue that GN-6 which results in a much more gradual release of

477   calcein, also could work through pore formation. The difference in kinetics of these peptides (GN-2

478   and GN-6) might be related to the lifetime of the pores [35, 38], the size of the pores and the number of

479   pores [38], all of which reflects on the release of the entrapped molecules from the LUVs. Even though

480   pore formation may seem the best mechanism of action of tested GN peptides, the possibility of

481   membrane disruption exploited by a mixture of different mechanism should not be excluded [39]. The

482   release of calcein for both peptides, GN-2 and GN-6, levels off over time (Figure 5B-C) and this type

483   of behavior has been reported to indicate transient pore formation during the initial insertion step into

484   the lipid bilayer [34].

485   In conclusion, based on the experimental data obtained in the current study the primary antibacterial

486   mechanism of action of GN-2 and GN-6 is associated with membrane permeabilization at high peptide

487   concentrations with different kinetics and potencies. At more moderate peptide concentrations it

488   appears that the peptides affect on metabolic disturbance, and further work is required to strengthen

489   these observations.

490

491   **Acknowledgements**

494   dynamic light scattering measurements of our liposomes, and Jacob Krake (Roskilde University) for

495   LC-MS analysis.

496

497   **References**

498   1.   Nathan, C., Antibiotics at the crossroads. *Nature* **2004,** *431* (7011), 899-902.
499   2.   von Nussbaum, F.; Brands, M.; Hinzen, B.; Weigand, S.; Habich, D., Antibacterial natural products in
500   medicinal chemistry--exodus or revival? *Angew Chem Int Ed Engl* **2006,** *45* (31), 5072-129.
501   3.   Klevens, R. M.; Morrison, M. A.; Nadle, J.; Petit, S.; Gershman, K.; Ray, S.; Harrison, L. H.; Lynfield, R.;
502   Dumyati, G.; Townes, J. M.; Craig, A. S.; Zell, E. R.; Fosheim, G. E.; McDougal, L. K.; Carey, R. B.; Fridkin, S. K.,
503   Invasive methicillin-resistant Staphylococcus aureus infections in the United States. *JAMA* **2007,** *298* (15),
504   1763-71.
505   4.   Fischbach, M. A.; Walsh, C. T., Antibiotics for emerging pathogens. *Science* **2009,** *325* (5944), 1089-93.
506   5.   Jenssen, H.; Hamill, P.; Hancock, R. E., Peptide antimicrobial agents. *Clin Microbiol Rev* **2006,** *19* (3), 491-
507   511.
508   6.   Hamill, P.; Brown, K.; Jenssen, H.; Hancock, R. E., Novel anti-infectives: is host defence the answer? *Curr*
509   *Opin Biotechnol* **2008,** *19* (6), 628-36.
510   7.   Hale, J. D.; Hancock, R. E., Alternative mechanisms of action of cationic antimicrobial peptides on bacteria.
511   *Expert Rev Anti Infect Ther* **2007,** *5* (6), 951-9.
512   8.   Jenssen, H.; Hancock, R. E., Antimicrobial properties of lactoferrin. *Biochimie* **2009,** *91* (1), 19-29.
513   9.   Wang, G.; Li, X.; Wang, Z., APD2: the updated antimicrobial peptide database and its application in peptide
514   design. *Nucleic Acids Res* **2009,** *37* (Database issue), D933-7.
515   10.   Fjell, C. D.; Jenssen, H.; Hilpert, K.; Cheung, W. A.; Pante, N.; Hancock, R. E.; Cherkasov, A., Identification of
516   novel antibacterial peptides by chemoinformatics and machine learning. *J Med Chem* **2009,** *52* (7), 2006-15.
517   11.   Godballe, T.; Nilsson, L. L.; Petersen, P. D.; Jenssen, H., Antimicrobial beta-peptides and alpha-peptoids.
518   *Chem Biol Drug Des* **2011,** *77* (2), 107-16.
519   12.   Fjell, C. D.; Jenssen, H.; Cheung, W. A.; Hancock, R. E.; Cherkasov, A., Optimization of antibacterial peptides
520   by genetic algorithms and cheminformatics. *Chem Biol Drug Des* **2011,** *77* (1), 48-56.
521   13.   Wiegand, I.; Hilpert, K.; Hancock, R. E., Agar and broth dilution methods to determine the minimal
522   inhibitory concentration (MIC) of antimicrobial substances. *Nat Protoc* **2008,** *3* (2), 163-75.
523   14.   (a) Falla, T. J.; Karunaratne, D. N.; Hancock, R. E. W., Mode of action of the antimicrobial peptide
524   indolicidin. *Journal of Biological Chemistry* **1996,** *271* (32), 19298-19303; (b) Selsted, M. E.; Novotny, M. J.;
525   Morris, W. L.; Tang, Y. Q.; Smith, W.; Cullor, J. S., Indolicidin, a novel bactericidal tridecapeptide amide from
526   neutrophils. *The Journal of biological chemistry* **1992,** *267* (7), 4292-5.
527   15.   Shai, Y., Mode of action of membrane active antimicrobial peptides. *Biopolymers* **2002,** *66* (4), 236-48.
528   16.   Russell, A. L.; Kennedy, A. M.; Spuches, A. M.; Venugopal, D.; Bhonsle, J. B.; Hicks, R. P., Spectroscopic and
529   thermodynamic evidence for antimicrobial peptide membrane selectivity. *Chem Phys Lipids* **2010,** *163* (6),
530   488-97.
531   17.   Greenfield, N. J., Using circular dichroism spectra to estimate protein secondary structure. *Nat Protoc* **2006,**
532   *1* (6), 2876-90.
533   18.   Whitmore, L.; Wallace, B. A., Protein secondary structure analyses from circular dichroism spectroscopy:
534   methods and reference databases. *Biopolymers* **2008,** *89* (5), 392-400.

535 19. (a) Bechinger, B., Structure and functions of channel-forming peptides: magainins, cecropins, melittin and
536   alamethicin. *The Journal of membrane biology* **1997,** *156* (3), 197-211; (b) Brogden, K. A., Antimicrobial
537   peptides: pore formers or metabolic inhibitors in bacteria? *Nature reviews. Microbiology* **2005,** *3* (3), 238-
538   50; (c) Wessman, P.; Stromstedt, A. A.; Malmsten, M.; Edwards, K., Melittin-lipid bilayer interactions and
539   the role of cholesterol. *Biophysical journal* **2008,** *95* (9), 4324-36.
540 20. (a) Chan, D. I.; Prenner, E. J.; Vogel, H. J., Tryptophan- and arginine-rich antimicrobial peptides: structures
541   and mechanisms of action. *Biochimica et biophysica acta* **2006,** *1758* (9), 1184-202; (b) Schibli, D. J.; Epand,
542   R. F.; Vogel, H. J.; Epand, R. M., Tryptophan-rich antimicrobial peptides: comparative properties and
543   membrane interactions. *Biochem Cell Biol* **2002,** *80* (5), 667-77.
544 21. Wadhwani, P.; Epand, R. F.; Heidenreich, N.; Burck, J.; Ulrich, A. S.; Epand, R. M., Membrane-active
545   peptides and the clustering of anionic lipids. *Biophysical journal* **2012,** *103* (2), 265-74.
546 22. Chen, Y.; Guarnieri, M. T.; Vasil, A. I.; Vasil, M. L.; Mant, C. T.; Hodges, R. S., Role of peptide hydrophobicity
547   in the mechanism of action of alpha-helical antimicrobial peptides. *Antimicrobial agents and chemotherapy*
548   **2007,** 51 (4), 1398-406.
549 23. Slaninova, J.; Mlsova, V.; Kroupova, H.; Alan, L.; Tumova, T.; Monincova, L.; Borovickova, L.; Fucik, V.;
550   Cerovsky, V., Toxicity study of antimicrobial peptides from wild bee venom and their analogs toward
551   mammalian normal and cancer cells. Peptides 2012, 33 (1), 18-26.
552 24. Eliassen, L. T.; Berge, G.; Leknessund, A.; Wikman, M.; Lindin, I.; Lokke, C.; Ponthan, F.; Johnsen, J. I.;
553   Sveinbjornsson, B.; Kogner, P.; Flaegstad, T.; Rekdal, O., The antimicrobial peptide, lactoferricin B, is
554   cytotoxic to neuroblastoma cells in vitro and inhibits xenograft growth in vivo. International journal of
555   cancer. Journal international du cancer 2006, 119 (3), 493-500.
556 25. Steen, H. B., Flow cytometry of bacteria: glimpses from the past with a view to the future. J Microbiol
557   Methods 2000, 42 (1), 65-74.
558 26. Pasotti, L.; Zucca, S.; Lupotto, M.; Cusella De Angelis, M. G.; Magni, P., Characterization of a synthetic
559   bacterial self-destruction device for programmed cell death and for recombinant proteins release. Journal
560   of biological engineering 2011, 5, 8.
561 27. Walberg, M.; Gaustad, P.; Steen, H. B., Rapid assessment of ceftazidime, ciprofloxacin, and gentamicin
562   susceptibility in exponentially-growing E. coli cells by means of flow cytometry. Cytometry 1997, 27 (2),
563   169-78.
564 28. Kohanski, M. A.; Dwyer, D. J.; Collins, J. J., How antibiotics kill bacteria: from targets to networks. Nature
565   reviews. Microbiology 2010, 8 (6), 423-35.
566 29. Galhardo, R. S.; Hastings, P. J.; Rosenberg, S. M., Mutation as a stress response and the regulation of
567   evolvability. Critical reviews in biochemistry and molecular biology 2007, 42 (5), 399-435.
568 30. Moussa, M.; Perrier-Cornet, J. M.; Gervais, P., Damage in Escherichia coli cells treated with a combination
569   of high hydrostatic pressure and subzero temperature. Appl Environ Microbiol 2007, 73 (20), 6508-18.
570 31. Stocks, S. M., Mechanism and use of the commercially available viability stain, BacLight. Cytometry A 2004,
571   61 (2), 189-95.
572 32. Huang, H. W., Molecular mechanism of antimicrobial peptides: the origin of cooperativity. Biochimica et
573   biophysica acta 2006, 1758 (9), 1292-302.
574 33. Spindler, E. C.; Hale, J. D.; Giddings, T. H., Jr.; Hancock, R. E.; Gill, R. T., Deciphering the mode of action of
575   the synthetic antimicrobial peptide Bac8c. Antimicrobial agents and chemotherapy 2011, 55 (4), 1706-16.
576 34. Hugonin, L.; Vukojevic, V.; Bakalkin, G.; Graslund, A., Membrane leakage induced by dynorphins. FEBS
577   letters 2006, 580 (13), 3201-5.
578 35. Arbuzova, A.; Schwarz, G., Pore-forming action of mastoparan peptides on liposomes: a quantitative
579   analysis. Biochimica et biophysica acta 1999, 1420 (1-2), 139-52.

580   36. (a) Irudayam, S. J.; Berkowitz, M. L., Influence of the arrangement and secondary structure of melittin
581   peptides on the formation and stability of toroidal pores. Biochimica et biophysica acta 2011, 1808 (9),
582   2258-66; (b) Sengupta, D.; Leontiadou, H.; Mark, A. E.; Marrink, S. J., Toroidal pores formed by
583   antimicrobial peptides show significant disorder. Biochim Biophys Acta 2008, 1778 (10), 2308-17.
584   37. Allende, D.; Simon, S. A.; McIntosh, T. J., Melittin-induced bilayer leakage depends on lipid material
585   properties: evidence for toroidal pores. Biophysical journal 2005, 88 (3), 1828-37.
586   38. Rex, S.; Schwarz, G., Quantitative studies on the melittin-induced leakage mechanism of lipid vesicles.
587   Biochemistry 1998, 37 (8), 2336-45.
588   39. (a) Pistolesi, S.; Pogni, R.; Feix, J. B., Membrane insertion and bilayer perturbation by antimicrobial peptide
589   CM15. Biophys J 2007, 93 (5), 1651-60; (b) Teixeira, V.; Feio, M. J.; Bastos, M., Role of lipids in the
590   interaction of antimicrobial peptides with membranes. Progress in lipid research 2012, 51 (2), 149-77.
591
592

A

B
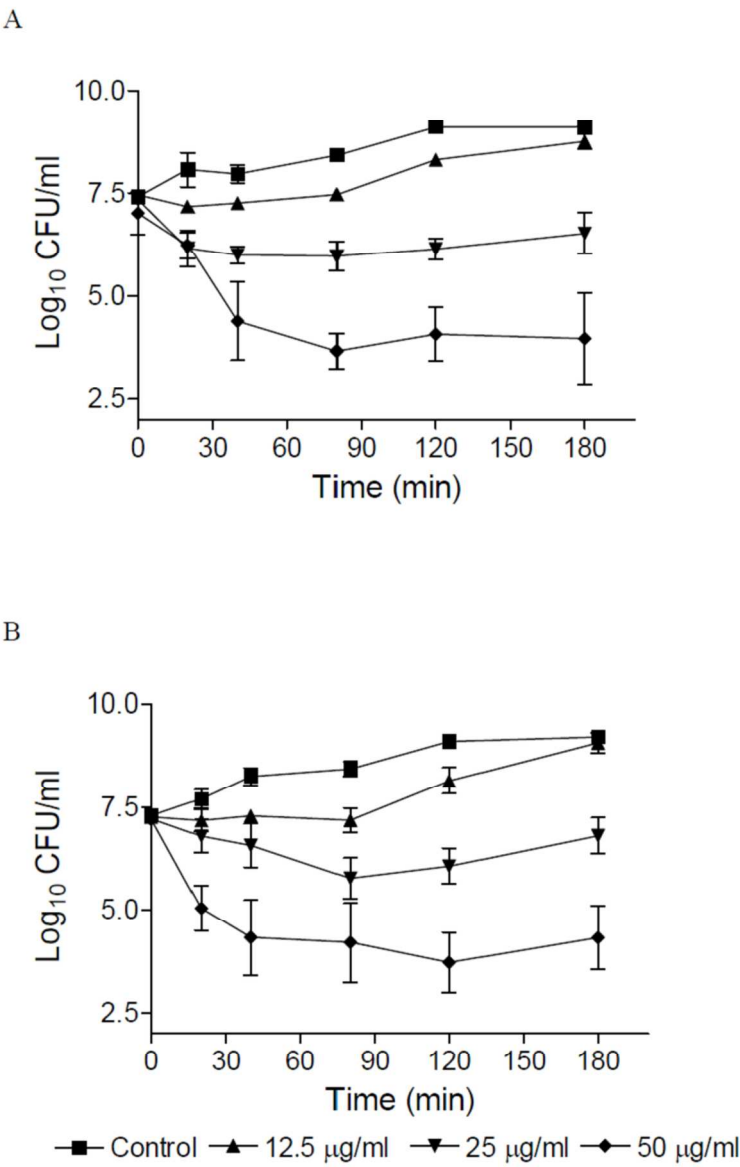

Figure 1. Viability of exponentially growing E. coli ATCC 25922 exposed to 1x, 2x, and 4x MIC concentrations of (A) GN-2 peptide and (B) GN-6 peptide over a course of 3 hours. Data represent mean and SEM of 3 independent experiments.
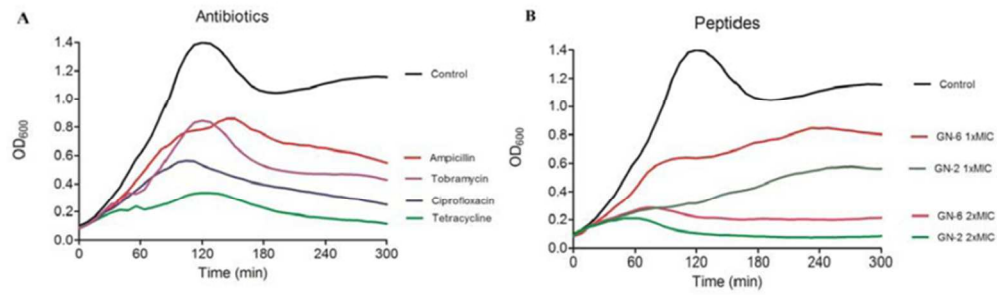97x148mm (600 x 600 DPI)

Figure 2. Optical density measurements of exponentially growing E. coli ATCC 25922 over 5 hours. Data presents mean of 3 independent experiments based. Bacterial growth at 37°C in a 96-well plates from a starting inoculum of OD600 of 0.1 has been measured with 8 minutes intervals. (A) Bacteria exposed to antibiotics at MIC concentrations, Ampicillin (4 µg/ml), Tobramycin (0.78 µg/ml), Tetracycline (1 µg/ml) and Ciprofloxacin (0.05 µg/ml). (B) Bacteria exposed to GN-2 peptide at 1x MIC (6.2 µg/ml) and 2x MIC (12.5 µg/ml) and GN-6 peptide at 1x MIC (12.5 µg/ml) and 2x MIC (25 µg/ml) concentrations.
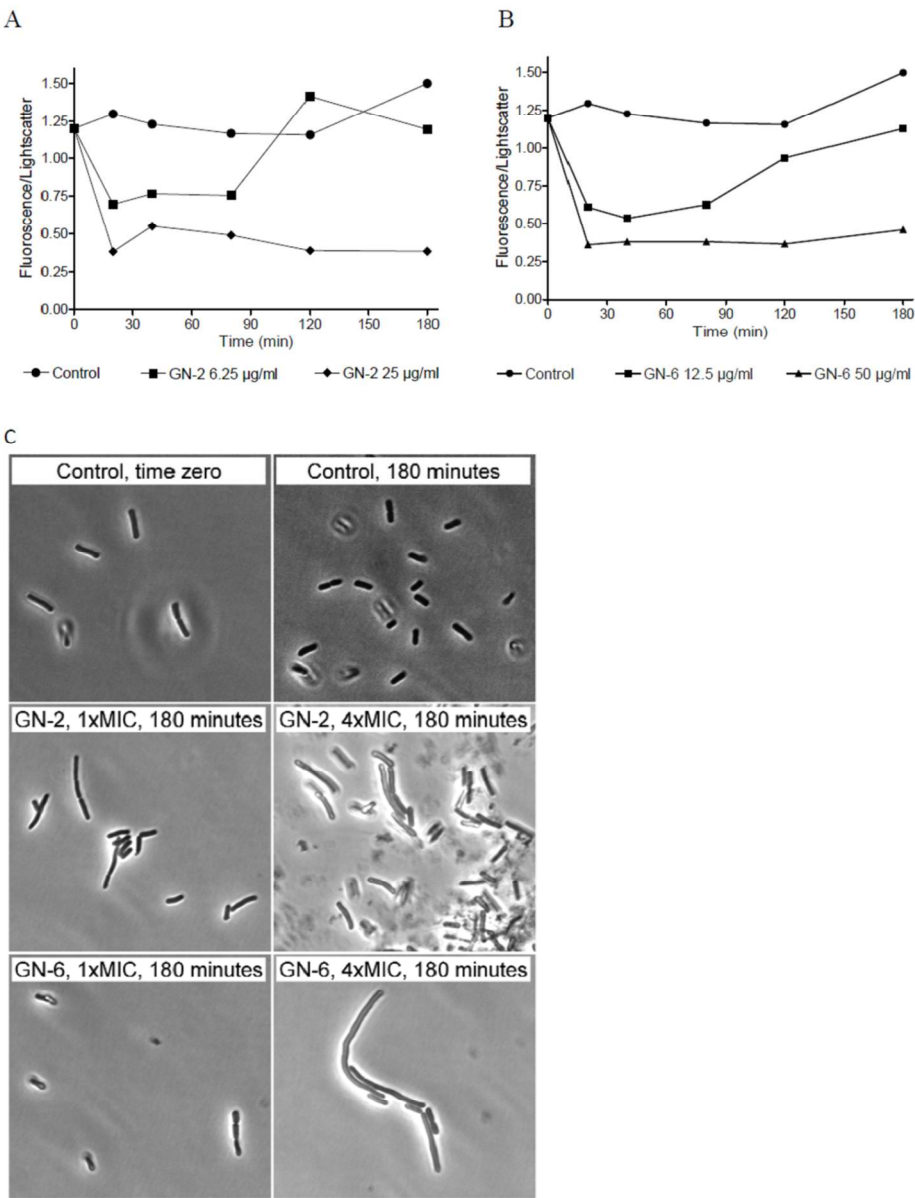42x12mm (600 x 600 DPI)

A

B

C

Figure 3. Peptide effect on E. coli morphology. (A,B) Flow cytometry data of GN-2 and GN-6 peptide influence on the DNA content per cell mass represented by fluorescence/lightscatter ratio, respectively. Data collected over a course of 3 hours in a microtitter plate format with an inoculum of OD600 of 0.1 and incubated at 37°C between extractions. (C) Microscope images of ethanol stained flow cytometry samples of E. coli treated with GN-2 and GN-6 peptide at 1x and 4xMIC concentration for 3 hours. Bacteria without cellular content appear transparent. Pictures taken at same magnification with a Leica DM5000 B microscope.
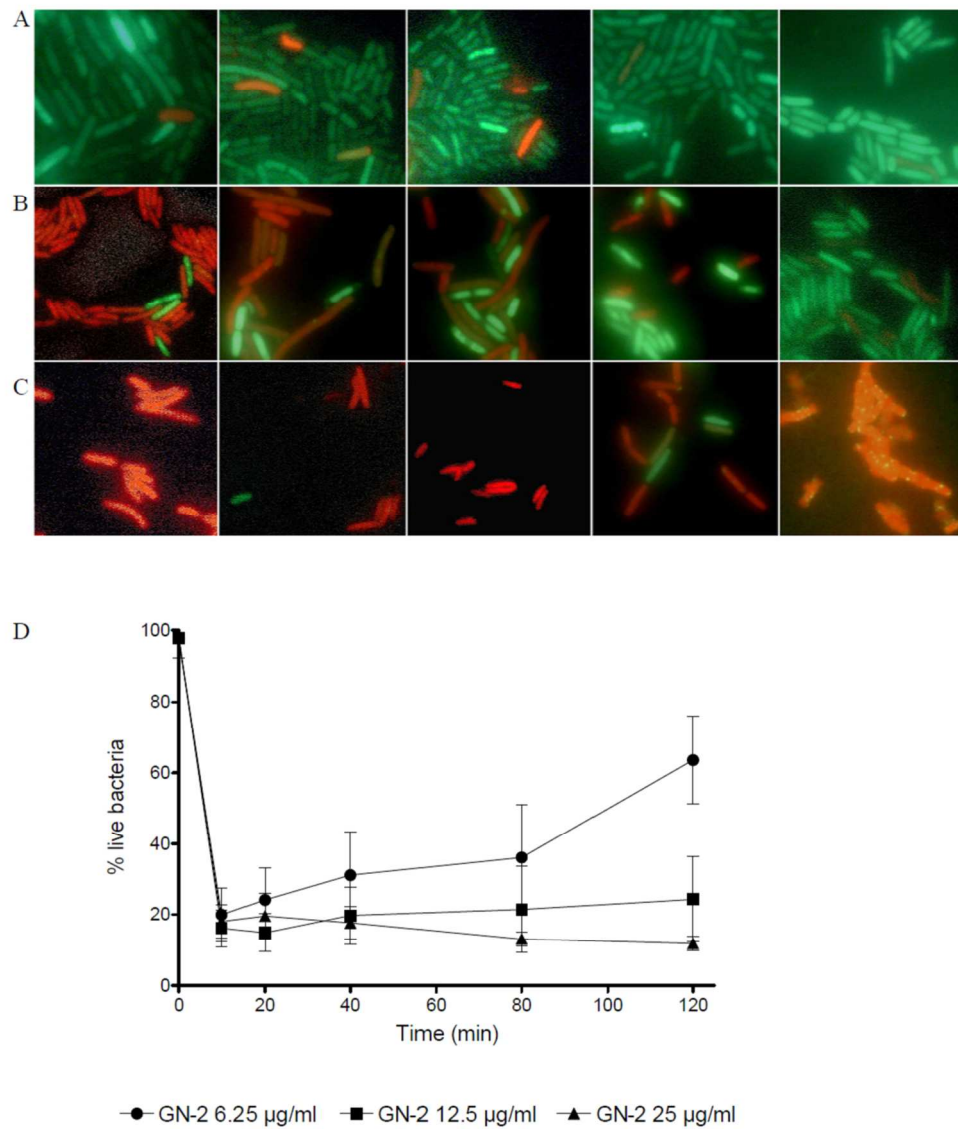87x113mm (600 x 600 DPI)

Figure 4. Visualization and quantification of membrane permeabilization of GN-2 peptide on E. coli ATCC 25922 over a period of 120 minutes. (A) Control cells. (B) Bacteria exposed to 1xMIC GN-2 peptide. (C) Bacteria exposed to 4xMIC GN-2 peptide. (D) Percentage of live bacteria after treatment with 1x, 2x and 4xMIC concentration of peptide GN-2. Pictures taken with Leica DM5000B microscope using mercury lamp. 118x138mm (600 x 600 DPI)
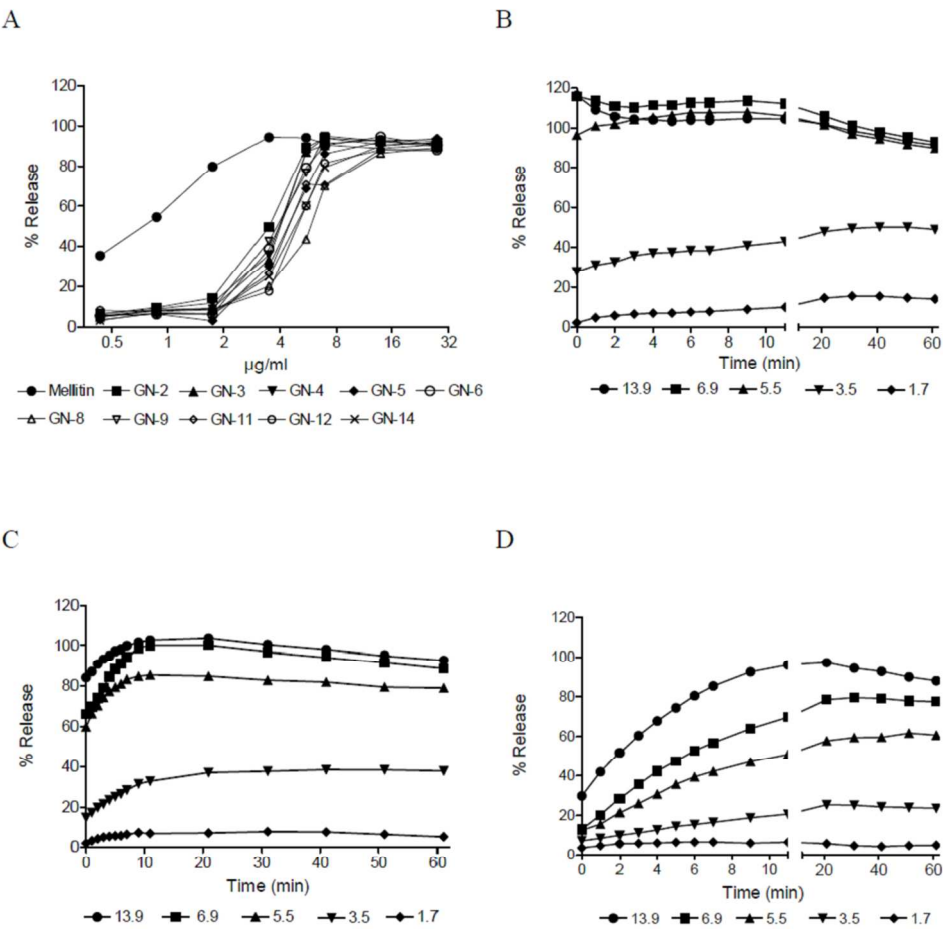
Figure 5. Calcein release from POPG:POPC vesicles. (A) Calcein leakage measurements from 20 µM POPG:POPC (7:3) vesicles at 37°C at various peptide concentrations in a 96-well format assay at 60 min. All readings are baseline corrected by subtracting values from wells containing only liposomes. 100% leakage is estimated as a total calcein release from liposomes exposed to 10 % Triton X-100. Represented results are mean values of three independent experiments with good reproducibility. Standard error bars are omitted for clarity. Calcein leakage measurements from 20 µM POPG:POPC (7:3) vesicles at 37°C at various concentrations of (B) GN-2, (C) GN-6 and (D) GN-14, in a 96-well format assay over a period of 1 hour.
76x74mm (600 x 600 DPI)

Table 1. Peptide characteristics, antimicrobial activity and toxicity

Peptide	Sequence	HPLC retention-time (min)	Hydrophobic moment	Minimal Inhibitory Concentration (μg/ml)			< 10 % Hemolysis	IC50
				E. coli	*P. aeruginosa*	*S. aureus*		
GN-2	RWKRWWRWI-CONH₂	6.33	5.4	6.2	3.1	3.1	100	47
GN-3	KWWRWRRWW-CONH₂	6.62	3.3	12.5	25	6.2	100	106
GN-4	RWKKWWRWL-CONH₂	6.54	5.5	6.2	3.1	6.2	100	37
GN-5	KKRWWWWWR-CONH₂	7.10	2.8	12.5	6.2	1.5	100	131
GN-6	RKRWWWWFR-CONH₂	7.08	2.8	12.5	6.2	3.1	100	97
GN-8	IWKRWWWKR-CONH₂	4.54	2.2	25	100	50	> 400	199
GN-9	RIWKIWWKR-CONH₂	4.63	4.8	25	25	> 50	> 400	> 200
GN-11	IKWKRWWWR-CONH₂	5.88	3.4	12.5	50	25	> 400	> 200
GN-12	KWWKIWRWR-CONH₂	6.13	2.9	25	12.5	12.5	> 400	173
GN-14	RLWKRWWIR-CONH₂	4.43	4.4	6.2	100	25	100	> 200
Indolicidin	ILPWKWPWWPWRR-CONH₂	ND	1.2	25	100	12.5	100	> 200

Table 1: Hydrophobic moment is a quantitative measure of amphipathicity calculated with HydroMCalc using the CCS scale. Median MIC values of GN peptides in μg/ml against *E. coli* ATCC 25922, *P. aureginosa* PA01 and *S. aureus* ATCC 29213 obtained by 3 repeated experiments. Hemolysis values are the mean concentration in μg/ml recorded over 3 experiments that induced less than 10% hemolysis. IC50 values in μg/ml is a toxicity measurement resulting from the MTT assays performed on HeLa cells, and calculated from the equation Y=Bottom + (Top-Bottom)/(1+10^((LogIC50-X)*HillSlope)).

Figure 1. Viability of exponentially growing *E. coli* ATCC 25922 exposed to 1x, 2x, and 4x MIC concentrations of (**A**) GN-2 peptide and (**B**) GN-6 peptide over a course of 3 hours. Data represent mean and SEM of 3 independent experiments.

Figure 2. Optical density measurements of exponentially growing *E. coli* ATCC 25922 over 5 hours. Data presents mean of 3 independent experiments based. Bacterial growth at 37°C in a 96-well plates from a starting inoculum of OD_{600} of 0.1 has been measured with 8 minutes intervals. (**A**) Bacteria exposed to antibiotics at MIC concentrations, Ampicillin (4 µg/ml), Tobramycin (0.78 µg/ml), Tetracycline (1 µg/ml) and Ciprofloxacin (0.05 µg/ml). (**B**) Bacteria exposed to GN-2 peptide at 1x MIC (6.2 µg/ml) and 2x MIC (12.5 µg/ml) and GN-6 peptide at 1x MIC (12.5 µg/ml) and 2x MIC (25 µg/ml) concentrations.

Figure 3. Peptide effect on *E. coli* morphology. (**A,B**) Flow cytometry data of GN-2 and GN-6 peptide influence on the DNA content per cell mass represented by fluorescence/lightscatter ratio, respectively. Data collected over a course of 3 hours in a microtitter plate format with an inoculum of OD_{600} of 0.1 and incubated at 37°C between extractions. (**C**) Microscope images of ethanol stained flow cytometry samples of *E. coli* treated with GN-2 and GN-6 peptide at 1x and 4xMIC concentration for 3 hours. Bacteria without cellular content appear transparent. Pictures taken at same magnification with a Leica DM5000 B microscope.

Figure 4. Visualization and quantification of membrane permeabilization of GN-2 peptide on *E. coli* ATCC 25922 over a period of 120 minutes. (**A**) Control cells. (**B**) Bacteria exposed to 1xMIC GN-2 peptide. (**C**) Bacteria exposed to 4xMIC GN-2 peptide. (**D**) Percentage of live bacteria after treatment with 1x, 2x and 4xMIC concentration of peptide GN-2. Pictures taken with Leica DM5000B microscope using mercury lamp.

Figure 5. Calcein release from POPG:POPC vesicles. (**A**) Calcein leakage measurements from 20 µM POPG:POPC (7:3) vesicles at 37°C at various peptide concentrations in a 96-well format assay at 60 min. All readings are baseline corrected by subtracting values from wells containing only liposomes. 100% leakage is estimated as a total calcein release from liposomes exposed to 10 % Triton X-100. Represented results are mean values of three independent experiments with good reproducibility. Standard error bars are omitted for clarity. Calcein leakage measurements from 20

µM POPG:POPC (7:3) vesicles at 37°C at various concentrations of (**B**) GN-2, (**C**) GN-6 and (**D**) GN-14, in a 96-well format assay over a period of 1 hour.